Electronic Supplementary Information (ESI†)

Ionothermal Template Transformations for Preparation of Tubular Porous Nitrogen Doped Carbons

J. Pampel*, A. Mehmood, M. Antonietti, and T.-P. Fellinger*

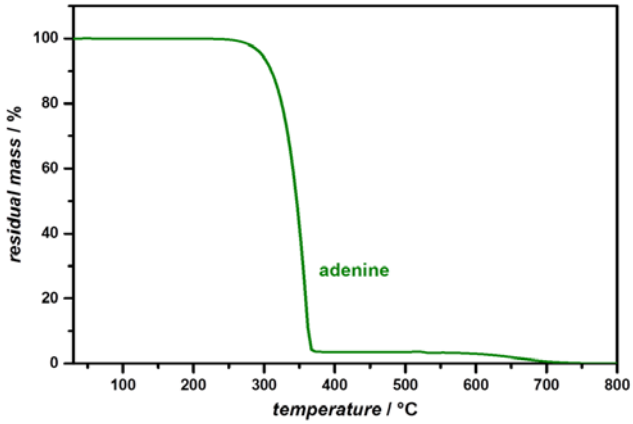

Fig. S1 Thermogravimetric analysis of the thermal decomposition of adenine in inert gas atmosphere.

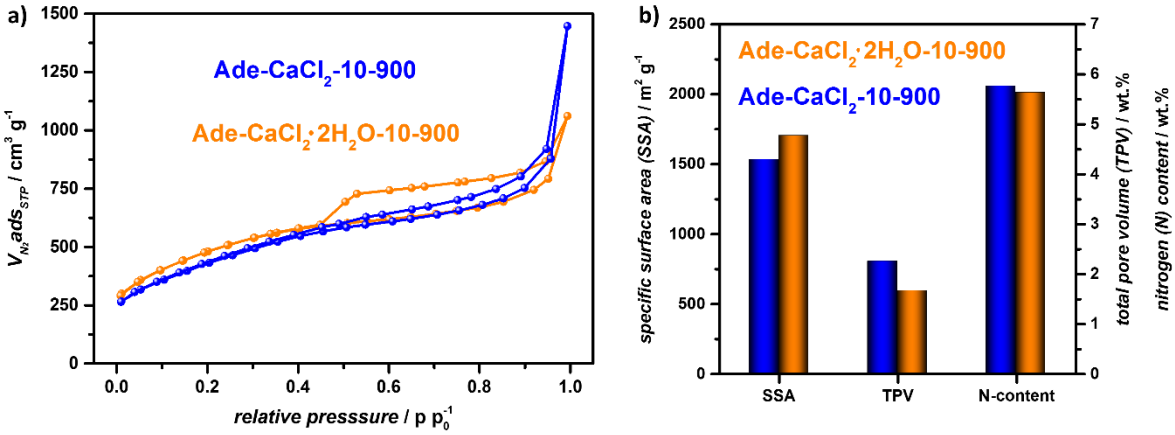

Fig. S2 a) Nitrogen physisorption isotherms and b) SSA, TPV, and N-content of adenine derived NDCs using either $CaCl_2$ or $CaCl_2 \cdot 2\ H_2O$ as salt. The precursor to salt wt.-ratio was fixed to 1:10 in both cases.

$CaCl_2$ results in a composite isotherm of type I(b) and type III coupled with a small H3 hysteresis pointing to micropores and a high amount of large interstitial pores. Contrarily, the isotherm of Ade-$CaCl_2 \cdot 2\ H_2O$ can be described as type I(b) with a H4 hysteresis showing less N_2 uptake at high pressures. This indicates that the application of $CaCl_2 \cdot 2\ H_2O$ promotes the general miscibility of adenine and salt phase leading to smaller pores which can also explain the ~ 10 % higher SSA in the case of the hydrated salt.

Table S1 Different characteristics of Ade-$CaCl_2$-10-900 and Ade-$CaCl_2 \cdot 2\ H_2O$-10-900: specific surface area and total pore volume obtained from nitrogen physisorption, elemental composition (C, H, N) obtained by combustion analysis, and calculated carbon yield as well as total yield.

sample	SSA_{BET} / $m^2\ g^{-1}$	$TPV_{p/po = 0.99}$ / $cm^3\ g^{-1}$	*C – content* / wt.%	*H – content* / wt.%	*N – content* / wt.%	*carbon yield* / %	*total yield* / %
Ade-$CaCl_2$-10-900	1530	2.24	76.5	1.7	5.8	15.6	9.0
Ade-$CaCl_2 \cdot 2\ H_2O$-10-900	1700	1.65	85.8	1.5	5.6	25.7	13.3

Apparently, the hydrated form of $CaCl_2$ supports the fixation of gaseous decomposition products of adenine which points to a molten state of the salt during initial adenine crosslinking. The very low carbon yield of the Ade-$CaCl_2$-10-900 points to adenine decomposition in manner of a solid-state reaction. Hence, the carbonization takes place on the surface of the solid $CaCl_2$ particles which goes along with the graphene like morphology observed by SEM and TEM (Fig. S3a+b).

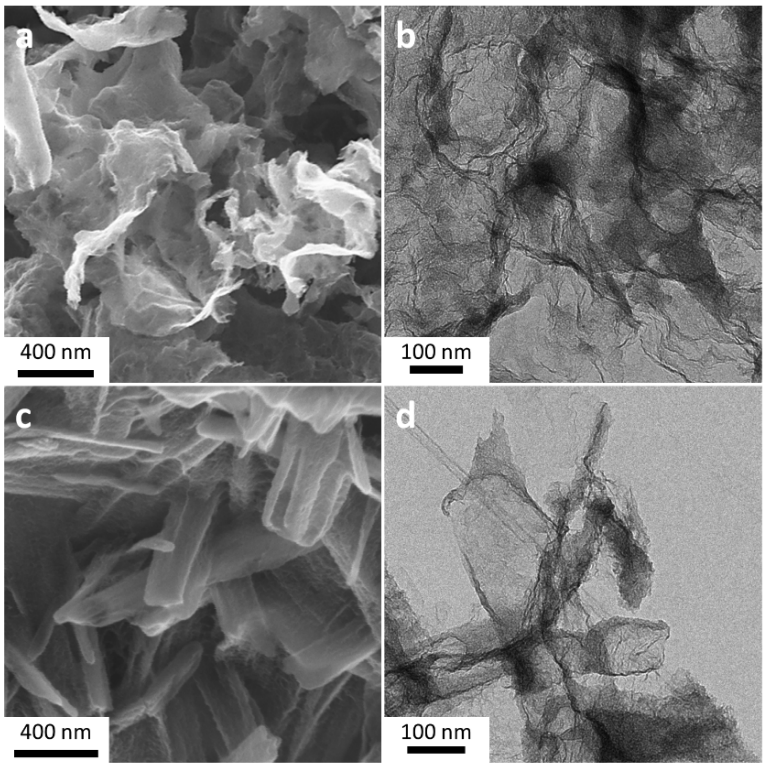

Fig. S3 a) SEM and b) TEM image of Ade-$CaCl_2$-10-900. c) SEM and d) TEM image of Ade-$CaCl_2 \cdot 2\ H_2O$-10-900.

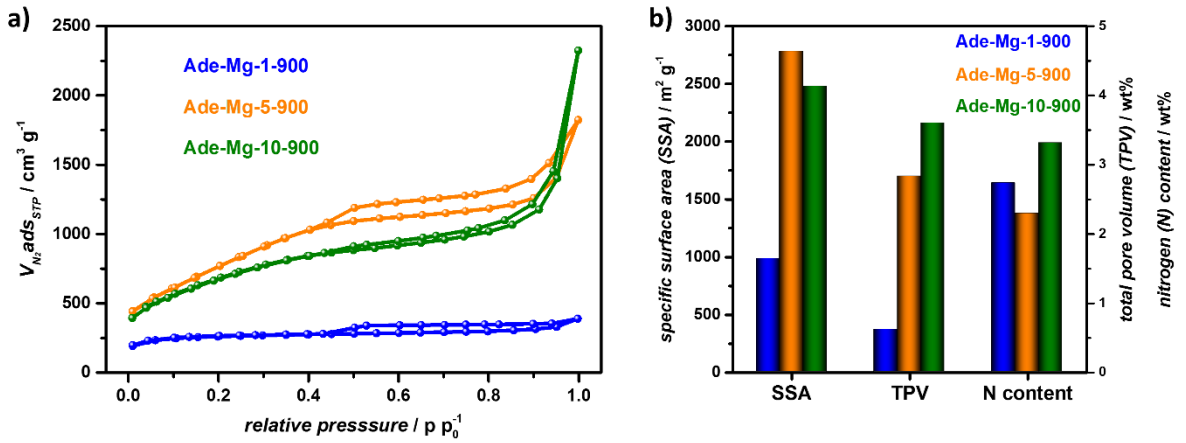

Fig. S4 a) Nitrogen physisorption isotherms and b) SSA, TPV, and N-content of Ade-Mg-1-900, Ade-Mg-5-900 and Ade-Mg-10-900

Table S2. Different characteristics of Ade-Mg-1-900, Ade-Mg-5-900, and Ade-Mg-10-900: surface area and total pore volume obtained from nitrogen physisorption, elemental composition (C, H, N) obtained by combustion analysis, and calculated carbon yield as well as total yield.

sample	SSA_{BET} / $m^2\ g^{-1}$	$TPV_{p/po = 0.99}$ / $cm^3\ g^{-1}$	*C – content* / wt.%	*H – content* / wt.%	*N – content* / wt.%	*carbon yield* / %	*total yield* / %
Ade-Mg-1-900	980	0.61	80.0	1.6	2.7	17	10.8
Ade-Mg-5-900	2780	2.83	88.3	1.3	2.3	25.6	13.7
Ade-Mg-10-900	2480	3.60	85.4	1.3	3.3	26.4	13.8

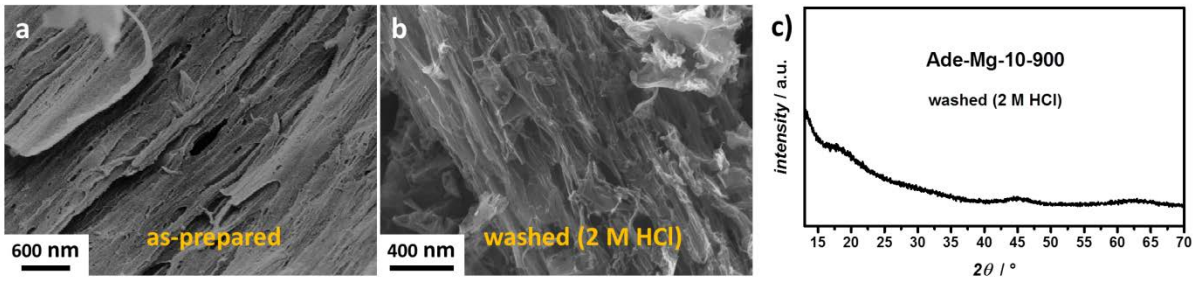

Fig. S5 a) SEM image of Ade-Mg-10-900_as-prepared, b) SEM image of Ade-Mg-10-900 (after acidic work-up), and c) PXRD of Ade-Mg-10-900 (after acidic work-up).

Any influence of the work-up on the morphology can be excluded as SEM reveals the fibrous domains already in the unwashed material. Moreover, all (crystalline) inorganic species are completely removed during the final washing in 2 M HCl.

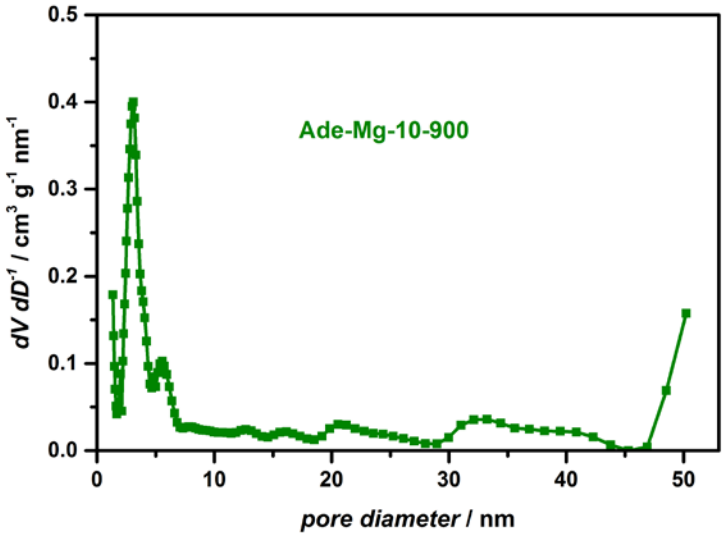

Fig. S6 Pore size distribution of Ade-Mg-10-900.

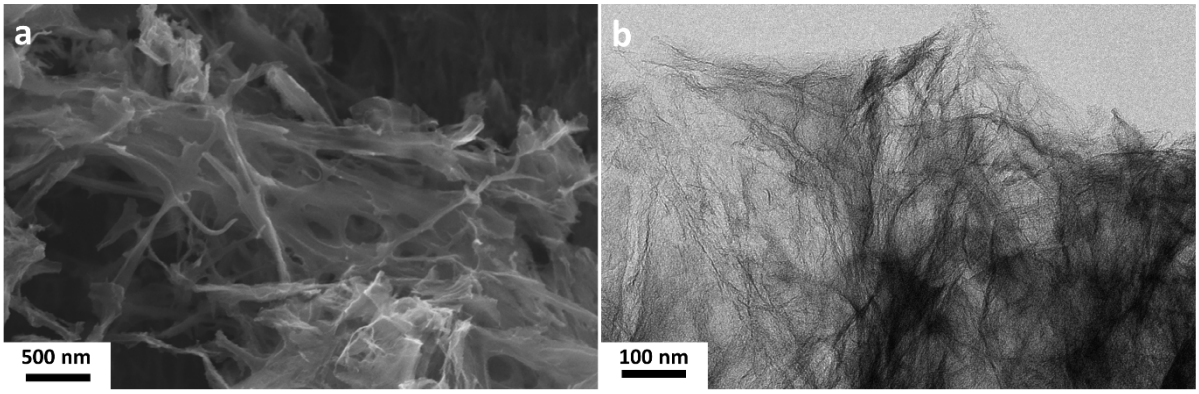

Fig. S7 a) SEM and b) TEM image of Ade-Mg-10-900 depicting a region with randomly oriented pores.

Table S3 Different characteristics of the Ade-Mg-10-X samples (X represents different synthesis temperatures): surface area and total pore volume obtained from nitrogen physisorption, elemental composition (C, H, N) obtained by combustion analysis, and calculated carbon yield as well as total yield.

sample	SSA_{BET} / $m^2 g^{-1}$	$TPV_{p/po = 0.99}$ / $cm^3 g^{-1}$	*C – content* / wt.%	*H – content* / wt.%	*N – content* / wt.%	*carbon yield* / %	*total yield* / %
Ade-Mg-10-500	35	0.13	47.6	3.4	31	-	-
Ade-Mg-10-600	700	0.88	49.1	3.3	27.1	-	-
Ade-Mg-10-700	1380	1.60	55.0	2.5	26.0	34.1	29
Ade-Mg-10-800	2680	3.42	68.21	2.4	15.4	29.4	19.2
Ade-Mg-10-875	2490	3.68	83.56	1.5	5.3	25.9	13.8
Ade-Mg-10-900	2480	3.60	85.43	1.3	3.31	26.4	13.8
Ade-Mg-10-925	2500	3.67	86.9	1.5	2.45	26.8	13.7
Ade-Mg-10-1000	2230	3.67	88.17	1.2	2.04	28.2	14.2

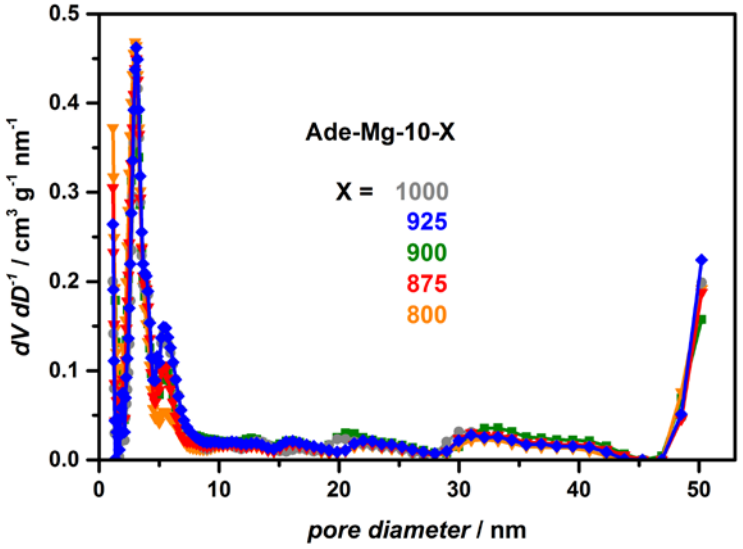

Fig. S8 Pore size distribution of the Ade-Mg-10 samples prepared at different synthesis temperatures.

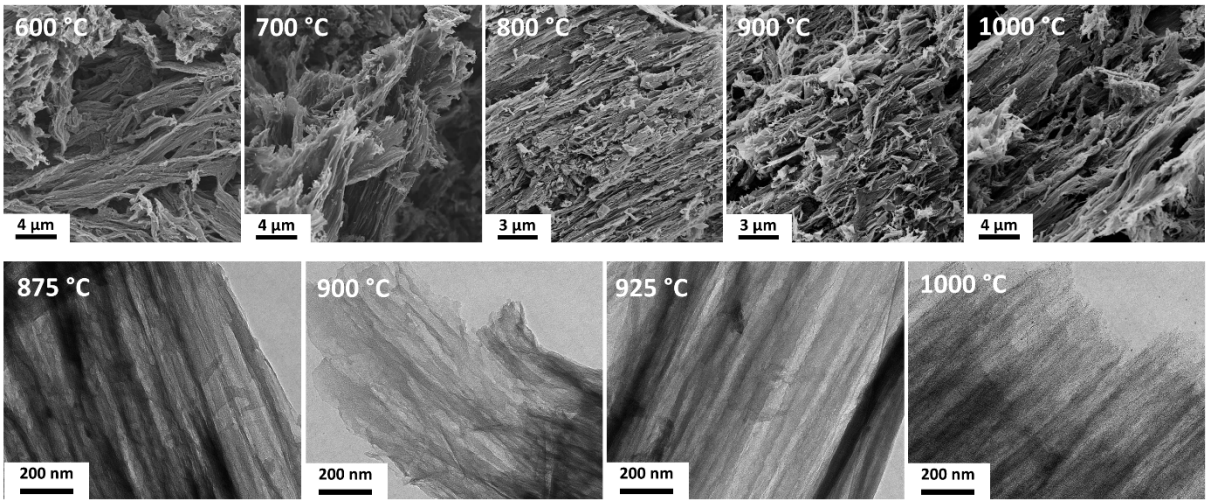

Fig. S9 Representative SEM images (upper row) and TEM images (lower row) of the Ade-Mg-10-X samples (X represents the synthesis temperature and is given in the respective image).

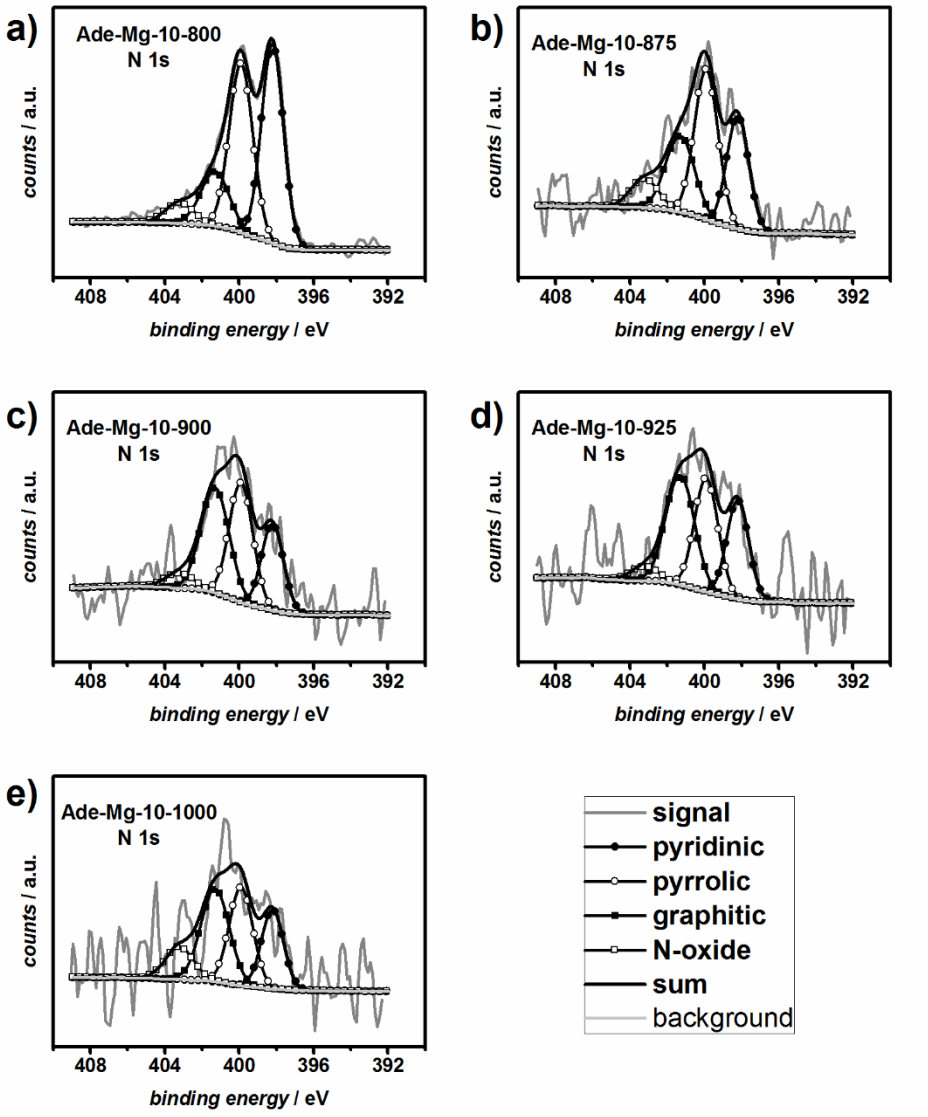

Fig. S10 N1s XPS spectra of the Ade-Mg-10 samples prepared at different synthesis temperatures. a) Ade-Mg-10-800, b) Ade-Mg-10-875, c) Ade-Mg-10-900, d) Ade-Mg-10-925, e) Ade-Mg-10-1000. Deconvoluted nitrogen peaks: pyridinic-N (398.2 eV); pyrrolic-N (399.9 eV); graphitic-N (401.3 eV), oxidized-N (403.2 eV).

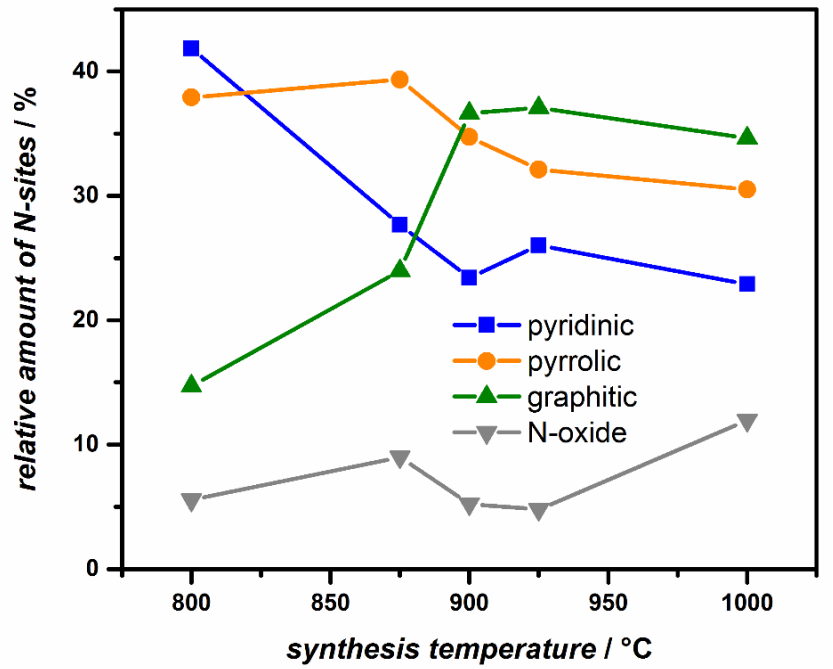

Fig. S11 Relative amount of N-sites of the Ade-Mg-10 samples prepared at different synthesis temperatures (quantified by XPS).

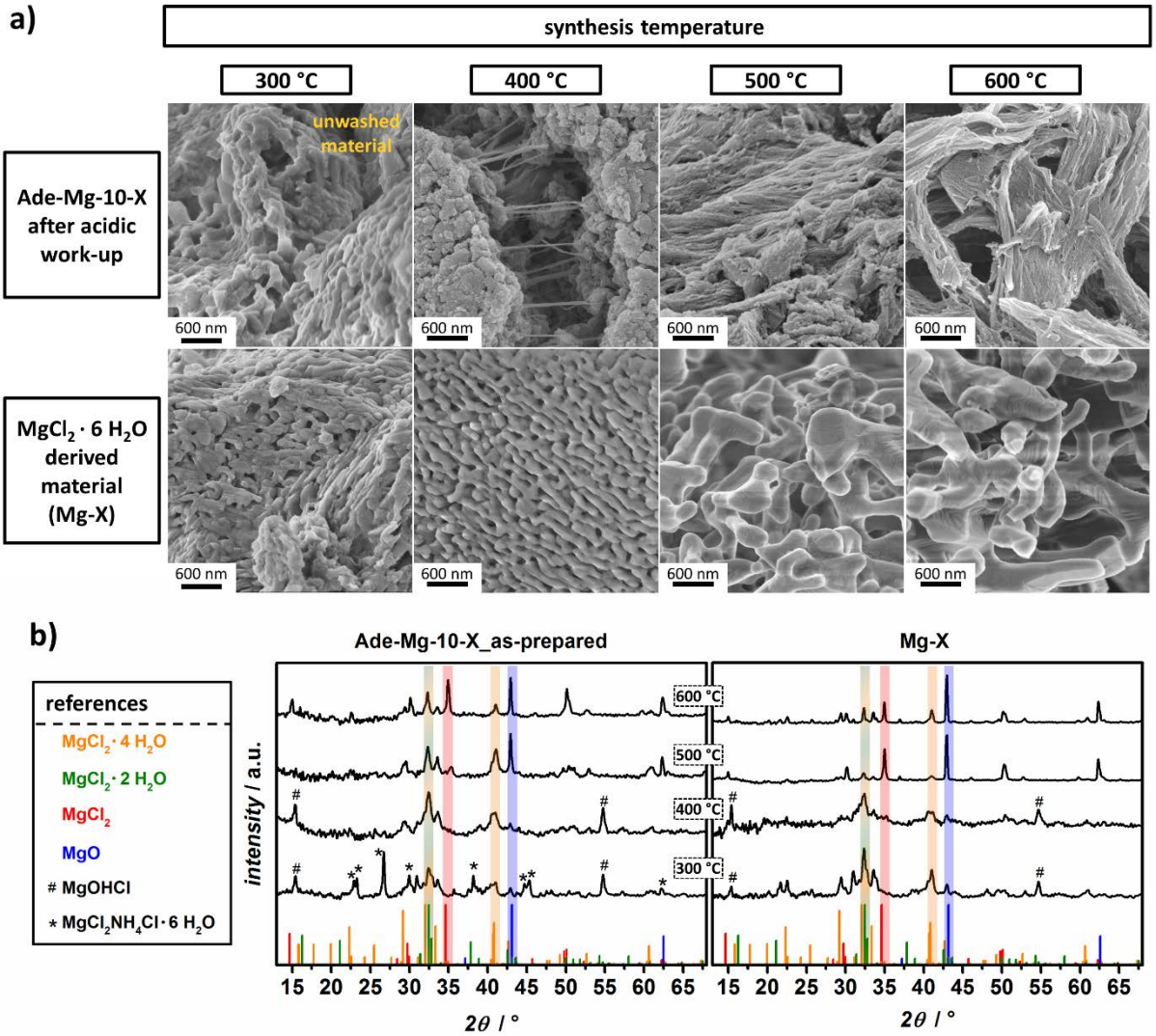

Fig. S12 a) SEM images of the Ade-Mg-10-X samples (upper row) and of the $MgCl_2 \cdot 6\,H_2O$ derived materials (bottom row) synthesized at different temperatures (300 – 600 °C). Ade-Mg-10-300 dissolved completely during the acidic work-up indicating that only small or instable adenine crosslinked pre-NDC domains were formed at such a low temperature. b) Normalized PXRD diffractograms of the corresponding unwashed materials (ICDD numbers of the references are given in Table S4).

Table S4 ICDD numbers of the PXRD reference patterns.

substance	*ICDD number*
MgO	04-016-6275
$MgCl_2$	04-008-7748
$MgCl_2 \cdot 2\ H_2O$	00-061-0221
$MgCl_2 \cdot 4\ H_2O$	04-015-2200
Mg(OH)Cl	00-003-0100
$MgCl_2NH_4Cl \cdot 6\ H_2O$	01-080-5969

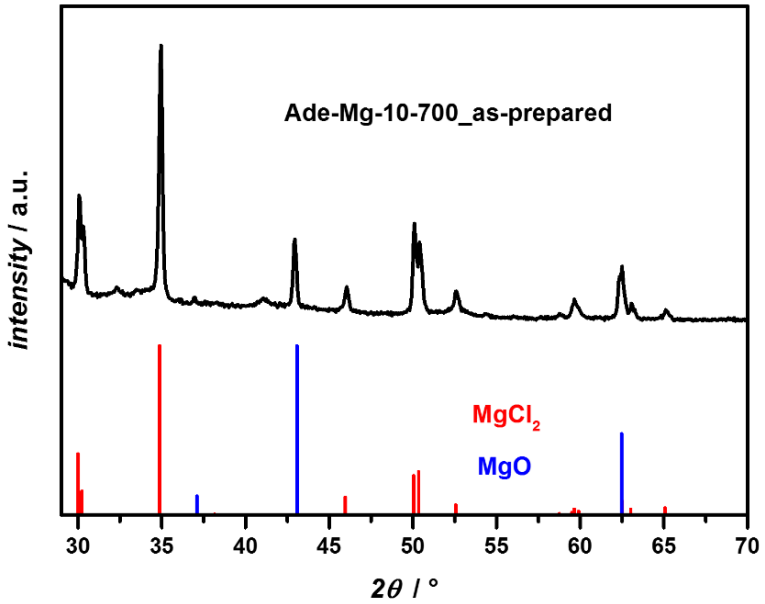

Fig. S13 a) PXRD of Ade-Mg-10-700_as-prepared (the ICDD numbers of the PXRD can be found in Table S4).

It is to consider that $MgCl_2$ is highly hygroscopic causing water uptake during the grinding of the material after the synthesis and during the PXRD measurements under ambient conditions. Thus, all unwashed (_as-prepared and Mg-X) samples were protected with amorphous tape to avoid the hydration during the PXRD measurements.

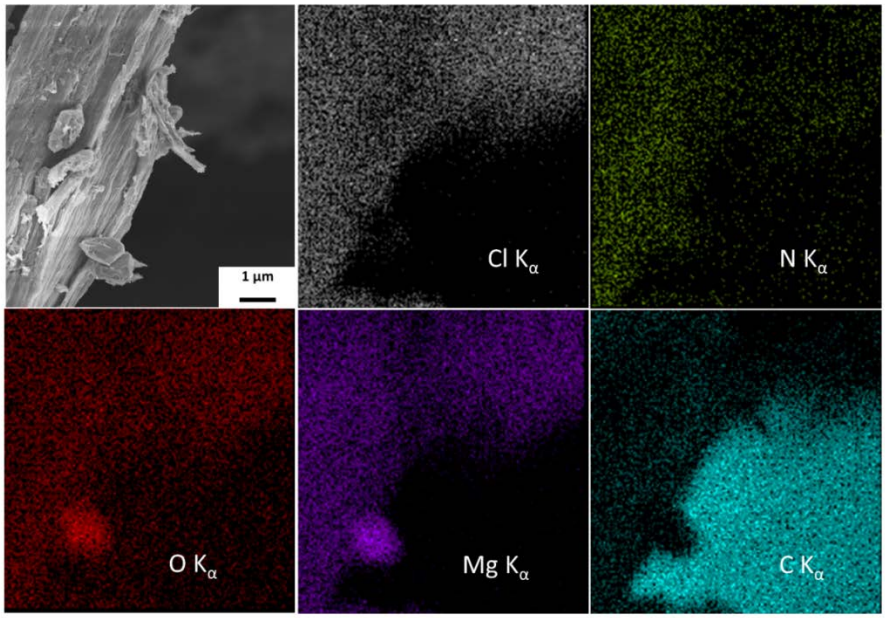

Fig. S14 EDX analysis (elemental mapping) of Ade-Mg-10-700_as prepared. The inverse contrast of the C K_α-signal is caused by the carbon tape of the SEM holder.

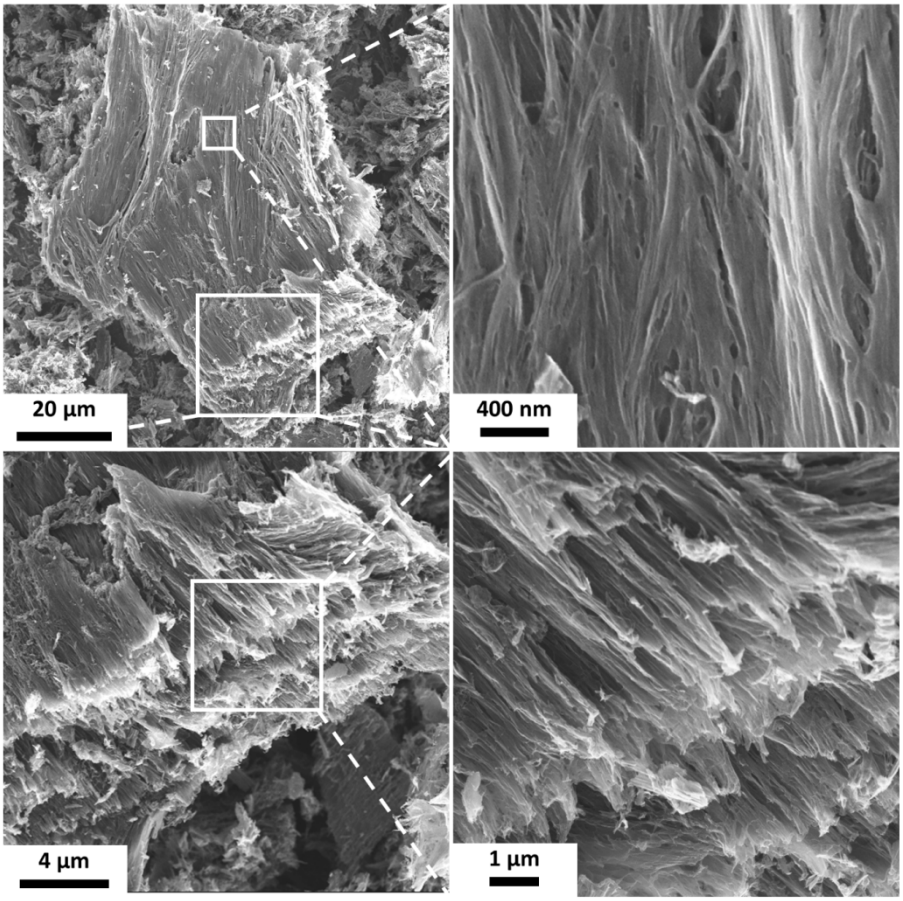

Fig. S15 SEM images with different magnifications of the material synthesized in the same fashion as Ade-Mg-10-900 but with an additional isothermal heating at 400 °C for ten hours during the typically used heating procedure. The images show the possibility to obtain large areas of fibrous NDC containing very long tubular pores.

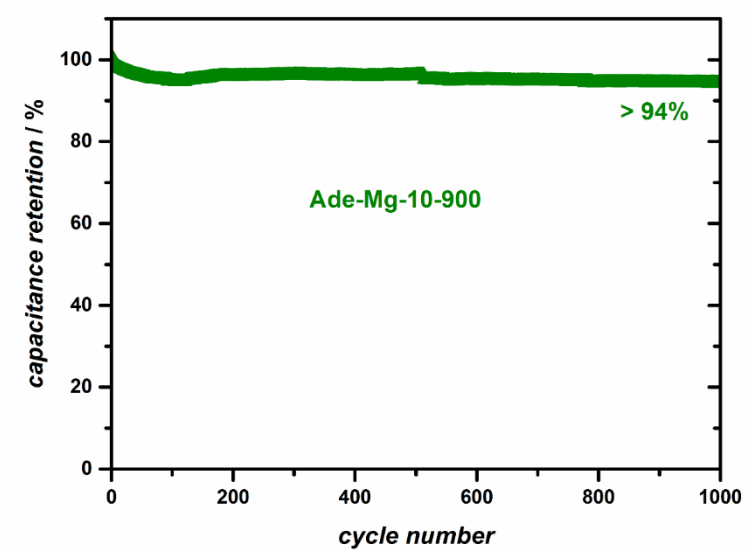

Fig. S16 Capacitance retention of Ade-Mg-10-900 in a two electrode set-up employing a constant charge/discharge current of 10 A g^{-1}.